Power Loss Reduction for MMSE-THP With Multidimensional Symbol Scaling

Adrian Garcia-Rodriguez, *Student Member, IEEE*, and Christos Masouros, *Senior Member, IEEE*

Abstract—This letter presents a strategy to reduce the power consumption of the Tomlinson–Harashima precoder (THP) based on the minimum mean square error (MMSE) criterion for the multi-user transmission. We show that a significant power loss reduction can be obtained by optimizing the interference to be cancelled by THP, using appropriate scaling of the interfering symbols. We advance the state of the art, by adopting a multi-dimensional optimization across a number of users and further modifying this optimization to apply to MMSE-THP, where it was previously inapplicable. By use of these improvements, the proposed approach is able to maintain or increase the error performance of MMSE-THP while providing up to 50% reduction in the power consumption.

Index Terms—Multi-user MIMO, Tomlinson–Harashima precoding, minimum mean square error, power loss.

I. INTRODUCTION

PRECODING techniques have been introduced as a feasible alternative to reduce the complexity at the mobile devices in the downlink of multi-user multiple-input multiple-output (MU-MIMO) scenarios [1]. In this setting, linear precoding schemes have been explored as a low-complexity solution to pre-cancel the interference at the transmitter [1], [2]. Alternatively, nonlinear precoding techniques are able to improve the performance of linear precoding algorithms by increasing their computational complexity [1], [3]. In this paper, we focus on Tomlinson–Harashima precoding (THP), a nonlinear technique that offers a compromise between performance and complexity [1]. THP eliminates interference by sequentially pre-subtracting the interfering symbols at the transmitter. The zero forcing (ZF) THP fully eliminates interference at the cost of enhancing the pre-detection noise while the MMSE-THP approach improves performance by maximizing the signal to interference plus noise ratio (SINR). Both approaches lead to an increase in the transmit power with respect to (w.r.t.) the case without precoding commonly referred to as power loss.

The power loss is originated by the energy difference between the original constellation symbols and the symbols that are transmitted after the THP operation. To reduce this harmful effect, complex domain interference optimized THP (CIO-THP) and power-efficient THP (PE-THP) focus on ZF-THP and propose to adaptively scale the user constellation symbols, provided that signal-to-noise ratio (SNR) constraints are met at the receivers [3], [4]. These constraints guarantee that the average system performance of conventional THP is not damaged
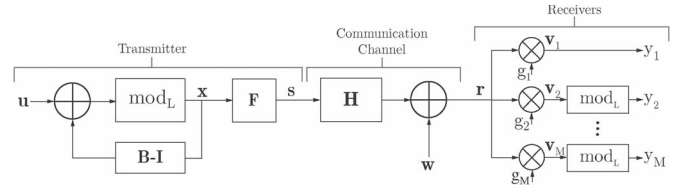
Fig. 1. Block diagram.

by the difference in amplitude and phase of the user symbols. As a result of optimizing the interference, the power spent on interference cancellation is reduced.

In this letter, we non-trivially extend the power loss reduction offered by CIO-THP and PE-THP to the MMSE criterion for THP, where it was previously inapplicable. The extension to MMSE-THP is non-trivial due to the variation in the constraints of the power minimization defined in [3], [4]. This variation is produced by their dependence on the number of optimized users and the interfering signals that the MMSE solution inherently allows [3]. The differences in the behavior of the power loss and the bit error rates produced by these adjustments are the subject of analysis of this work.

II. MULTIDIMENSIONAL INTERFERENCE OPTIMIZED MMSE-THP (MMSE-MIO-THP)

A. The MU-MIMO Transmission Model

The model assumed hereafter is a multi-user MIMO downlink system comprised of M single-antenna users served by one base station with $N > M$ antennas. In general, this setting can be described by

$$\mathbf{r} = \mathbf{H}\mathbf{s} + \mathbf{w}, \qquad (1)$$

where $\mathbf{s} \in \mathbb{C}^{N \times 1}$ represents the transmit symbols and $\mathbf{w} \in \mathbb{C}^{M \times 1} \sim \mathcal{CN}(0, \sigma_n^2 \mathbf{I}_M)$ is the additive white Gaussian noise (AWGN) with variance σ_n^2. Moreover, $\mathbf{r} \in \mathbb{C}^{M \times 1}$ is the vector of received symbols and $\mathbf{H} \in \mathbb{C}^{M \times N}$ refers to the channel matrix. In the following, we assume a frequency flat Rayleigh fading channel $\mathbf{H}$ with independent, identically distributed, circularly symmetric complex normal entries [1], [2].

B. Proposed MMSE-MIO-THP

The proposed scheme employs a MMSE-THP precoder as shown in Fig. 1. The precoding operation is a function of the lower triangular matrix $\mathbf{R}$, which reads as the solution of the Cholesky decomposition of the channel [5]

$$\mathbf{R} = \text{chol}\left[(\mathbf{H}\mathbf{H}^H + \xi\mathbf{I}_M)\mathbf{H}^{-H}\mathbf{H}^{-1}(\mathbf{H}\mathbf{H}^H + \xi\mathbf{I}_M)\right]. \quad (2)$$

In the above, $(\cdot)^H$ denotes the Hermitian transpose, $\xi = \sigma_n^2/\sigma_s^2$, and σ_s^2 refers to the variance of the signal transmitted by the
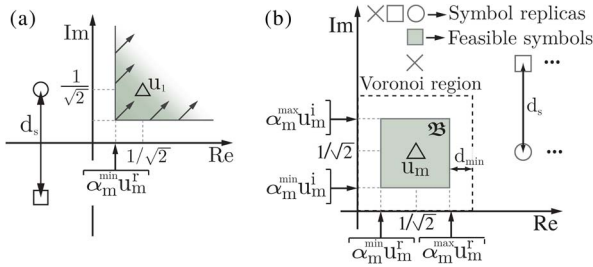
Fig. 2. Optimization constraints and regions with the feasible scaled constellation symbols for (a) CIO-MMSE-THP and (b) MIO-MMSE-THP for users $2 < n < K$.

nth antenna, s_n, provided that $\mathbb{E}[\mathbf{s}^H\mathbf{s}] = \sigma_s^2\mathbf{I}_N$. In THP, the transmitter sends the signal $\mathbf{s} = \mathbf{Fx}$, where $\mathbf{F}$ is a unitary matrix defined as $\mathbf{F} = \mathbf{H}^{-1}(\mathbf{H}\mathbf{H}^H + \xi\mathbf{I}_M)\mathbf{R}^{-H}$ [5]. For the proposed scheme, the elements of $\mathbf{x}$ are given as

$$x_m(\hat{\boldsymbol{\alpha}}_m) = \left[\tilde{u}_m - \sum_{l=1}^{m-1} b_{m,l}x_l(\hat{\boldsymbol{\alpha}}_l)\right] \text{mod}_L, \quad m \in [1, M],$$
(3)

where $\hat{\boldsymbol{\alpha}}_m$ and $\tilde{u}_m$ are the scaling factors and scaled information symbols, respectively as detailed in the next section, and $b_{m,l}$ are the entries of the lower left triangular matrix $\mathbf{B} = \mathbf{GR}$. In the previous expression, $\mathbf{G} = \text{diag}(\{\mathbf{R}\}_{i,i}^{-1})$ refers to the diagonal matrix that is applied at the receivers.

The modulo operation at the transmitter $[\cdot] \text{mod}_L$ constrains the transmit symbols within the Voronoi regions of the signal constellation and it introduces virtual constellation symbols that belong to an extended constellation as shown in Fig. 2(b). Moreover, we note that the variance σ_s^2 found in (2) is related to the power loss that THP systems have due to the application of the modulo operation. Therefore, the matrices $\mathbf{B}$, $\mathbf{G}$, and $\mathbf{F}$ are modified in the proposed technique w.r.t. THP due to the power loss reduction experienced by the adaptive symbol scaling. Finally, the output of the mth receiver is independent of the scaling performed at the transmitter and it reads as

$$y_1 = g_{1,1} \cdot r_1,$$
$$y_m = [g_{m,m} \cdot r_m]\, \text{mod}_L, \qquad \text{for } m \geq 2$$
(4)

where $g_{m,m}$ is the mth element of the diagonal of $\mathbf{G}$, and $\mathbf{r} = [r_1, r_2, \ldots, r_M]^T$ is the received signal before applying the scaling and modulo operations at the receivers.

In the following it has been assumed that the original data symbols u_n are selected from the Q-QAM constellation $\mathcal{A} = \{a_R + ia_I | a_R, a_I \in \{\pm1, \pm3, \ldots \pm(\sqrt{Q}-1)\}\}$. Moreover, the average energy of the constellation symbols is fixed to $\overline{E}_s = 1$ by normalizing with the coefficient $f_{nor} = \sqrt{2(Q-1)/3}$. The base L of the modulo operation is defined as $L = \sqrt{Q}/f_{nor}$.

C. Modified Interference Optimization

CIO-THP and PE-THP improve the power efficiency of conventional zero forcing THP by better aligning the interference to pre-subtract in the precoding process [3], [4]. The decrease in the total transmit power is achieved by adaptively scaling the user constellation symbols subject to performance thresholds at the receivers. In this letter we analyze the power loss reduction

when the interference optimization is applied to MMSE-THP. The modified constellation symbols $\tilde{u}_m$ are expressed as

$$\tilde{u}_m = \alpha_m^r u_m^r + i\alpha_m^i u_m^i, \qquad m \leq K$$
$$\tilde{u}_m = u_m, \qquad m > K$$
(5)

where $\alpha_m \triangleq \alpha_m^r + i\alpha_m^i$ is the scaling factor for the mth user with $\alpha_m^{\{r,i\}} \in \mathbb{R}^+$, and u_m is the mth element of the input vector $\mathbf{u}$. The precoded signal is then generated following (3).

The range of possible values that the scaling factors $\boldsymbol{\alpha} = [\alpha_1, \ldots, \alpha_K]^T$ can adopt must be bounded to guarantee a threshold performance [3], [4]. In particular, the bounds are a function of the error covariance matrix $\boldsymbol{\Theta}$ of the MMSE-THP solution [5]

$$\boldsymbol{\Theta} = \sigma_n^2\mathbf{G}\mathbf{G}^H + \sigma_n^2\xi\mathbf{G}(\mathbf{H}\mathbf{H}^H)^{-1}\mathbf{G}.$$
(6)

From (6), the expected SINR at the mth receiver Λ_m for modulations with equal symbol energy reads as

$$\Lambda_m = \frac{\left|\left(\hat{\alpha}_m u_m^r + i\hat{\alpha}_m u_m^i\right)\right|^2}{\Theta_{m,m}} = \frac{\overline{E}_s \cdot |\hat{\alpha}_m|^2}{\Theta_{m,m}},$$
(7)

where $\Theta_{m,m}$ is the mth element of the diagonal of the error covariance matrix $\boldsymbol{\Theta}$, and $\hat{\alpha}_m$ is the optimal of the real and imaginary scaling factors for the mth user. At this point, we note the dependence of the SINR on the power loss of the ZF systems via the $\xi = \sigma_n^2/\sigma_x^2$ factor included in the error covariance matrix. Hence, the power loss of the adaptive scaling techniques with the ZF criterion influences the optimization constraints of the MMSE solution, an aspect not considered in [3], [4].

The scaling factors for the proposed scheme that better align the interference with the symbols to transmit can be obtained by solving

$$\underset{\boldsymbol{\alpha}}{\text{minimize}} \quad \left\{\|\mathbf{x}\left[\boldsymbol{\alpha}(\boldsymbol{\lambda}, \boldsymbol{\Theta})\right]\|_2^2\right\}$$

$$\text{subject to} \quad \alpha_1^{\{r,i\}} \geq \alpha_1^{\min}$$

$$\alpha_m^{\min} \leq \alpha_m^{\{r,i\}} \leq \alpha_m^{\max} \text{ for } 2 \leq m \leq K,$$
(8)

where $\alpha_m^{\min}$ and $\alpha_m^{\max}$ are the lower and upper bounds of the linear optimization constraints as defined in the following, and $\boldsymbol{\lambda} = [\lambda_1, \ldots, \lambda_K]$ are the user-specified SINR thresholds that determine their performance. The above non-convex optimization problem can be re-expressed as a convex one, following the results in [3]. Specifically, as the direction of the interference to be eliminated at the transmitter remains known in advance, the conclusions achieved in [3] regarding the convexity of the problem also apply to the proposed strategy.

D. Optimization Constraints in MMSE-MIO-THP

The original zero forcing CIO-THP and PE-THP establish a threshold performance only based on the SNR requirements at the receivers. However, the interference that appears due to the use of the MMSE criterion must be considered in the proposed to ensure that the average performance is not damaged. From

MMSE-THP and MMSE-MIO-THP*	
Operation	*Complexity in flops*
$\mathbf{A} = \left(\mathbf{H}\mathbf{H}^H + \xi\mathbf{I}_M\right)\mathbf{H}^{-H}\mathbf{H}^{-1}\left(\mathbf{H}\mathbf{H}^H + \xi\mathbf{I}_M\right)$	$C_1 \simeq (104/3)\,N^3 - 16N^2 + 2N$
$\mathbf{R} = chol(\mathbf{A})$	$C_2 = (4/3)\,N^3 + 3N^2 + 2N$
$\mathbf{F} = \mathbf{H}^{-1}\left(\mathbf{H}\mathbf{H}^H + \xi\mathbf{I}_M\right)\mathbf{R}^{-H}$	$C_3 = (32/3)\,N^3 - 4N^2$
$\mathbf{\Theta} = \sigma_n^2\mathbf{G}^2 + \sigma_n^2\xi\mathbf{G}\mathbf{H}^{-H}\mathbf{H}^{-1}\mathbf{G}$	$C_4^* \simeq 8N^3$
Trust-Region-Reflective minimization [7]	$C_5^* = \mathcal{O}(2N \cdot S_{it})$
$S_{ev.\times}\begin{cases} \tilde{x}_m = \left[\tilde{u}_m - \sum_{l=1}^{m-1} b_{m,l}\tilde{x}_l\right]\mathrm{mod}_L, m \in 1\dots N \\ P_{tot} = \tilde{\mathbf{x}}^H \cdot \mathbf{x} \end{cases}$	$C_6^* \simeq S_{ev} \times (4N^2 + 11N)$
Total MMSE-THP	$C_{\mathrm{MMSE\text{-}THP}} \simeq (140/3)\,N^3 - 7N^2$
Total MMSE-MIO-THP	$C_{\mathrm{MMSE\text{-}MIO\text{-}THP}} \simeq (164/3)\,N^3 + (4S_{ev} - 7)\,N^2 + (11S_{ev} + 3)\,N$

(7), the lower bounds of the scaling factors of user $m \leq K$ for the examples of BPSK and 4-QAM are obtained as

$$\alpha_m^{\min} = \sqrt{\frac{\lambda_m}{E_s}\left[\underbrace{\sigma_n^2\mathbf{G}^2}_{\text{noise}} + \underbrace{\sigma_n^2\xi\mathbf{G}(\mathbf{H}\mathbf{H}^H)^{-1}\mathbf{G}}_{\text{interference}}\right]_{m,m}}, \quad (9)$$

This set of constraints ensures that the average distance between the mth scaled symbol and the original symbols from the non-extended constellation is higher than a given threshold.

Additionally, upper bounds on the scaling factors must also be considered when multiple users are optimized. This is because the application of the modulo operation generates virtual symbols that impose new decision thresholds as shown in Fig. 2. Hence, to guarantee that the distance with the extended constellation symbols is also preserved under the presence of interference, the upper bounds of the scaling factors for the examples of BPSK and QPSK must satisfy

$$\alpha_m^{\max} = 2 - \sqrt{\frac{\lambda_m}{E_s}\left[\underbrace{\sigma_n^2\mathbf{G}^2}_{\text{noise}} + \underbrace{\sigma_n^2\xi\mathbf{G}(\mathbf{H}\mathbf{H}^H)^{-1}\mathbf{G}}_{\text{interference}}\right]_{m,m}}. \quad (10)$$

The constraints defined in (9) and (10) ensure that the set of feasible constellation symbols is constrained in a square around the original symbols as represented in Fig. 2(b) by the shaded region, thus guaranteeing the SINR requirements at the receivers. Analytically, the minimum distance between a constellation symbol and the limits of its Voronoi region $d_{\min}$ satisfies

$$d_{\min} = \min\left[\Re(\mathcal{B})\right] = \min\left[\Im(\mathcal{B})\right] = \alpha^{\min}u^r = \alpha^{\min}u^i, \quad (11)$$

where $\mathcal{B}$ is the set of possible transmit symbols solution to (8). We note that, similarly to [4], the SINR thresholds can be selected so that the average performance is not degraded w.r.t. MMSE-THP [4]. These thresholds are defined as $\boldsymbol{\lambda} = \boldsymbol{\lambda}_A$. Further, extension of higher-order modulations is straightforward by considering the distance between symbols d_s [4].

III. POWER CONSUMPTION

To evaluate the true power savings achieved, the total power consumption of the communication system is modeled as [6]

$$P = P_{PA} + p_c \cdot C + N \cdot P_0. \quad (12)$$

Here, $P_{PA} = ((\nu/\eta) - 1)P_{\text{out}}$ accounts for the power consumption of a power amplifier to transmit a signal of $P_{\text{out}} = P_{\text{in}} \times P_{\text{loss}}$ Watts. In the previous expressions, P_{loss} denotes the power loss, P_{in} is the input power, ν is the peak to average power ratio (PAPR) of the selected modulation and η refers to the efficiency of the power amplifier [6]. The term $p_c \cdot C$ is the power required by a digital signal processor (DSP) that consumes p_c Watts/KFlops and implements a signal processing algorithm with average complexity C in elementary floating points operations. Moreover, P_0 refers to the power consumed by the circuitry of the RF chains and it is approximated as $P_0 = 34.4$ mW per antenna [6].

A. Complexity Analysis

To compute the complexity C in number of real floating points operations, in Table I we analyze the number of operations that must be performed in the proposed technique. For simplicity reasons, it is assumed that multiplications and divisions have the same complexity of summations and subtractions. Additionally, it has been considered that all useful partial results can be used in the subsequent operations.

The main difference in multidimensional scaling techniques compared to standard THP is the optimization problem defined in (8). The solution to the minimization process is obtained by solving a nonlinear least squares problem whose complexity analysis can be divided into two parts [7]. The first part corresponds to the operations involved in the minimization algorithm itself with a known complexity of $\mathcal{O}(S_{it} \cdot S_{par})$ for the Trust-Region-Reflective algorithm [7]. Here, S_{it} represents the number of iterations and S_{par} is the number of parameters to optimize. In this case, the total number of iterations is problem-dependent whereas number of parameters to optimize is $S_{par} = 2$ K. The second term refers to the complexity of evaluating S_{ev} times the function to minimize. We also note that a low-resolution search is performed before the execution of the above-mentioned algorithm to provide the required starting point. This process is not considered in the complexity analysis as it is only necessary when the symbol replicas of the optimal solution vary w.r.t. MMSE-THP [3]. At this point, we also remark the additional complexity load required when the MMSE criterion is used instead of the ZF one, cf. [4]. In Table I, the additional operations introduced by the proposed technique are pointed out by an asterisk. It can be observed that the additional complexity of the proposed is related to the need of computing
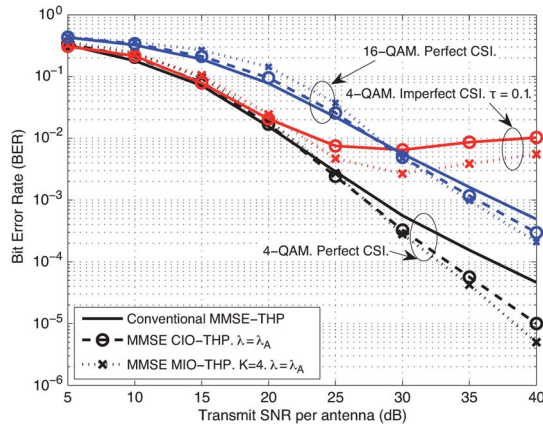
Fig. 3.   Bit error rate (BER) vs. transmit SNR per antenna for THP, CIO-THP and MIO-THP systems with $N = M = 4$ antennas. 4-QAM and 16-QAM.

the covariance matrix to determine the optimization constraints (C_4^*) and solving the optimization problem $(C_{5,6}^*)$.

IV. SIMULATION RESULTS

Monte Carlo simulations have been performed to characterize the performance and power-related aspects of the THP, CIO-THP and MIO-THP systems based on the MMSE criterion. The simulation setup is comprised of a transmitter with 4-QAM and 16-QAM modulations and a flat Rayleigh fading channel scenario. We note that the receivers' structure is the same for all schemes as no additional information is required when using the proposed technique. The transmitter employs a class-A amplifier with $\nu = 0.35$ [6], and the DSP is a Virtex-5 FPGA from Xilinx with $p_c = 5.76$ mW/KFlops [3]. The average transmit SNR per antenna is defined as $\text{SNR}_{\text{ant}} = \overline{E}_s/N_0$. Moreover, the Trust-Region-Reflective algorithm allows extracting the average number of iterations and function evaluations needed to estimate the complexity term of the total power consumption.

Fig. 3 shows the performance of the THP, CIO-THP and MIO-THP algorithms as a function of the transmit SNR per antenna in a system with $N = M = 4$ and $\boldsymbol{\lambda} = \boldsymbol{\lambda}_A$ for both perfect and imperfect CSI. The imperfect CSI follows the model used in [8], where $\tau \in [0, 1]$ regulates the accuracy of the CSI varying from perfect CSI ($\tau = 0$) to completely inaccurate CSI ($\tau = 1$). In this figure, it can be observed that the performance of the proposed approach resembles the one of MMSE-THP at low and intermediate SNRs whereas it outperforms the previous approaches at high SNRs. This effect is specially noticeable for 4-QAM and it is produced by the power loss reduction introduced by the ZF solutions, which in turn alter the definitions of the MMSE precoding matrices in (2). We also note that a similar error floor is experienced by all the techniques under study with imperfect CSI.

The power loss is depicted in Fig. 4(a) for the systems considered in this paper, a transmit SNR per antenna of 30 dB, and varying SNR thresholds. This figure shows that the benefits of the proposed technique in terms of power loss grow when the received SNR thresholds are reduced or a higher number of users are optimized. This is because better solutions to the optimization problem (8) can be obtained in these circumstances due to a wider range of feasible scaling factors. The total power consumption is depicted in Fig. 4(b) for a varying transmit SNR per antenna and $P_{\text{in}} = 1$ W. The difference in the power
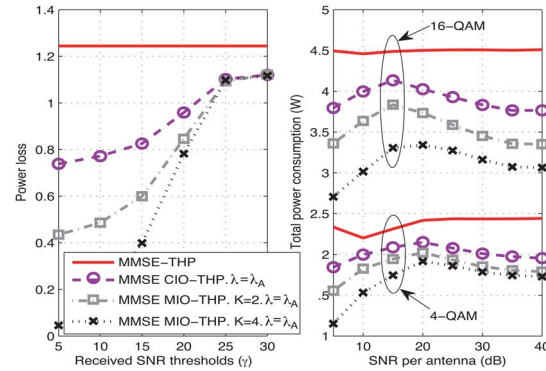

Fig. 4.   (a) Power loss vs. receive SNR thresholds (4-QAM) and (b) total power consumption vs. transmit SNR per antenna for THP, CIO-THP and MIO-THP systems with $N = M = 4$. 4-QAM and 16-QAM.

consumption between 4-QAM and 16-QAM is produced by the worse PAPR of the latter in the expression of P_{PA} in (12). Further, note that the trend of the power consumption differs from the one in [4] due to the different criterion and constraints of MMSE MIO-THP. Under the same conditions of Fig. 3, it can be seen that the proposed technique is able to achieve up to 50% reduction in the power consumption with higher performance than MMSE-THP.

V. CONCLUSION

A multidimensional interference optimization by means of symbol scaling has been analyzed in this letter for the MMSE-THP. Particularly, a redefinition of the interference optimization process to minimize the power loss has been developed to apply the optimization to multiple users as well as accounting for the interfering signals to satisfy a threshold performance at the receivers. Moreover, the specific modifications of the MMSE-THP matrices and the additional signal processing load have been studied in this work. The presented results show a substantial decrease in the power loss while maintaining or improving the performance of MMSE-THP.

REFERENCES

[1] C. Windpassinger, R. F. H. Fischer, T. Vencel, and J. Huber, "Precoding in multiantenna and multiuser communications," *IEEE Trans. Wireless Commun.*, vol. 3, no. 4, pp. 1305–1316, Jul. 2004.

[2] C. Peel, B. Hochwald, and A. Swindlehurst, "A vector-perturbation technique for near-capacity multiantenna multiuser communication-Part I: Channel inversion and regularization," *IEEE Trans. Commun.*, vol. 53, no. 1, pp. 195–202, Jan. 2005.

[3] C. Masouros, M. Sellathurai, and T. Ratnarajah, "Interference optimization for transmit power reduction in Tomlinson-Harashima precoded MIMO downlinks," *IEEE Trans. Signal Process.*, vol. 60, no. 5, pp. 2470–2481, 2012.

[4] A. Garcia-Rodriguez and C. Masouros, "Power-efficient Tomlinson-Harashima precoding for the downlink of multi-user MISO systems," *IEEE Trans. Commun.*, vol. 62, no. 6, pp. 1884–1896, Jun. 2014.

[5] J. Liu and W. Kizymien, "Improved Tomlinson-Harashima precoding for the downlink of multi-user MIMO systems," *Can. J. Elect. Comput. Eng.*, vol. 32, no. 3, pp. 133–144, 2007.

[6] S. Cui, A. Goldsmith, and A. Bahai, "Energy-constrained modulation optimization," *IEEE Trans. Wireless Commun.*, vol. 4, no. 5, pp. 2349–2360, Sep. 2005.

[7] K. Dufková, J.-Y. Le Boudec, L. Kencl, and M. Bjelica, "Predicting user-cell association in cellular networks from tracked data," in *Mobile Entity Localization and Tracking in GPS-less Environments*. Berlin, Germany: Springer-Verlag, 2009, pp. 19–33.

[8] S. Wagner, R. Couillet, M. Debbah, and D. T. M. Slock, "Large system analysis of linear precoding in correlated MISO broadcast channels under limited feedback," *IEEE Trans. Inf. Theory*, vol. 58, no. 7, pp. 4509–4537, Jul. 2012.